Erraticity analysis of multiparticle production in nucleus-nucleus interactions at relativistic energies

Dipesh Chanda,[1] Malay Kumar Ghosh,[1] Amitabha Mukhopadhyay,[1] and Gurmukh Singh[2]
[1]*Physics Department, University of North Bengal, Siliguri-734430, Darjeeling, West Bengal, India*
[2]*Department of Physics, Canisius College, 2001 Main Street, Buffalo, New York 14208*
(Received 12 July 2004; published 14 March 2005)

Nonstatistical fluctuation in the angular distribution of charged particles produced in high-energy nucleus-nucleus interactions is investigated by using the technique of erraticity moments. Nuclear photographic emulsion data on secondary shower track emissions collected from ^{16}O-Ag/Br and ^{32}S-Ag/Br interactions, each at an incident momentum of 200 *A* GeV/*c*, are analyzed. A generalized scaling law between the erraticity moments and the phase-space partition number is established for both sets of data. Experimental values of erraticity parameters are compared with those obtained from event samples generated by the Lund Monte Carlo model FRITIOF and by simple random numbers. In each case simulated results substantially underestimate the extent of experimentally observed nonstatistical fluctuation.

DOI: 10.1103/PhysRevC.71.034904 PACS number(s): 25.75.−q, 25.70.Pq, 24.60.Ky

I. INTRODUCTION

Unusually large local fluctuations in particle density distribution observed in the JACEE events [1] indicated that the fluctuations were not merely statistical artifacts. In their pioneering work Bialas and Peschanski [2] showed that, if these fluctuations were Poisson distributed, sample-averaged factorial moments $\langle F_q \rangle$ of order q (a positive integer) become equal to the average of ordinary moments C_q of the corresponding dynamical distribution, irrespective of the nature of the latter. Bialas and Peschanski also showed that $\langle F_q \rangle$ anomalously scale with diminishing scale size of the phase space variable. This scaling behavior, technically termed as "intermittency," has so far been extensively and successfully studied in many high-energy experiments [3–7], and efforts have been made to interpret these fluctuations in terms of phase transition, production of shock waves and related phenomena, or simple cascading effects [8]. Though the factorial moments are capable of filtering out the dynamical part of the spatial fluctuation it should however be noted that when averaged over a large sample of events, they may lose information on the variation of such spatial fluctuations from event to event. For example, creation of an exotic state such as a quark-gluon plasma (QGP) may result in large spatial fluctuations in the density distribution of final state hadrons. This may happen only in some of the events, and not in the entire event sample under consideration. In the process of averaging, information on such large fluctuations may be smoothed out. Therefore, it becomes imperative to study the fluctuation of single-event factorial moments as well.

Recently Cao and Hwa [9,10] have proposed a scheme to investigate the event-to-event fluctuation of single-event factorial moments F_q^e with the help of a new set of moments called "erraticity" moments $C_{p,q}$, where p is any positive number. The erraticity moments, which also scale with phase-space partition size obeying a generalized power law, can be related to an entropy index μ_q that can adequately determine the chaotic nature of spatial fluctuations in event space. A positive nonvanishing value of μ_q denotes a wide distribution of F_q^e, and this implies that the spatial fluctuations are unpredictable from event to event. All events in a sample may have started with same initial conditions, but during the collision process each event may have evolved with a different strength of dynamical fluctuation. Thus, such chaotic behavior may be attributed to a different dynamical fluctuation strength in different events.

The scaling behavior of erraticity moments has so far been verified in several high-energy hadronic and nuclear interactions [11–15], but the reason for such chaotic fluctuations in event space has remained far from clear. Thus the problem has to be investigated by comparing experimental results with model calculations with probable mechanisms of particle production as input. Whereas in the case of hadronic interactions such comparisons do exist in the literature [10–13], for nucleus-nucleus interactions at high energy they are virtually nonexistent. The objectives of the present work are (i) to comprehensively investigate the erraticty characteristics of particle production in ^{16}O-Ag/Br interactions at 200 *A* GeV/*c*, (ii) to compare the results of ^{16}O-Ag/Br interactions with the results obtained earlier from ^{32}S-Ag/Br interactions at the same incident momentum per nucleon [15], and (iii) to compare experimentally obtained results with those obtained from the Lund Monte Carlo model FRITIOF for high-energy nucleus-nucleus interactions [16], as well as in some cases with those obtained by generating simple random numbers.

II. THE EXPERIMENT

Ilford G-5 nuclear photographic emulsion pellicles were horizontally exposed to beams of ^{16}O and ^{32}S ions obtained from the Super Proton Synchrotron (SPS) at CERN, each having an incident momentum of 200 *A* GeV/*c*. After the emulsion plates were washed, developed, and mounted, they were volume scanned by two independent observers, and samples of central and semicentral events were found. The emulsion plates have a sensitivity of about 20 grains per 100 μm, and each measures 18 cm $\times$ 7 cm $\times$ 600 μm. The scanning was performed at a total magnification of 300$\times$ using Leitz Metaloplan microscopes. Any interaction

occurring either within 20 μm from the top or from the bottom surface of the emulsion plate was eliminated from the event sample to reduce any chance of undercounting the number of tracks as well as to reduce any error in angle measurement of secondary tracks. The emission angle θ of each secondary track emanating from an interaction vertex was measured with respect to the incident projectile track. In an event measurement of angles, the counting of the number of tracks and determination of the category of a particular track were all done at a total magnification of 1500× using oil immersion objectives. According to the terminology of the nuclear photographic emulsion technique, tracks coming out of an interaction can be classified into four categories: shower tracks, gray tracks, black tracks, and projectile fragments, details of which can be found elsewhere [15,17]. Trivial sources of fluctuation, originating from variation in collision geometry or from the uncertainty in the mass number of target nuclei were taken care of. Both samples were chosen by imposing certain conditions on the number of heavy target fragments ($n_h > 8$) and the number of projectile fragments ($n_{pf} = 0$) in each event. Such criteria will ensure that (i) the mass number of the target nucleus, which is either an Ag ($A = 108$) or a Br ($A = 80$) nucleus in each case, does not widely differ from each other and (ii) total fragmentation of the incident nucleus has taken place in each interaction. In this way a sample of 195 sulfur nucleus-induced events and another sample of 280 oxygen nucleus-induced events were chosen for measurement of emission angle θ of the secondary shower tracks, which are caused by the singly charged produced hadrons moving with very high speed ($\beta \approx 0.8$).

In our sample of ^{32}S-Ag/Br events the average number of shower tracks is $\langle n_s \rangle = 217.79 \pm 6.16$, and that for the ^{16}O-Ag/Br events is $\langle n_s \rangle = 119.26 \pm 3.59$. These numbers do not include any shower track falling within the very forward cone of emission ($\theta \leqslant 0.01$ radi), where an admixture of charged mesons with singly charged projectile fragments (baryons) is possible. The rapidity of a particle additive under Lorentz boost is conventionally used to locate a particle in one-dimensional phase space. In contrast, the pseudorapidity η of a particle is directly related to its emission angle,

$$\eta = -\ln \tan \frac{\theta}{2}. \tag{1}$$

Pseudorapidity is a suitable replacement for the rapidity of a particle (i) when the rest mass of the particle can be comfortably neglected in comparison to its energy or momentum, which is the case for hadrons produced in such high-energy collisions, and (ii) when neither the energy nor the momentum can be measured very easily, as is the case for nuclear emulsions. The uncertainty in the emission angle measurement was estimated to result in an accuracy ≈0.1 unit of pseudorapidity for particles falling within the region of present analysis.

As mentioned earlier the experimental results have also been compared with those obtained from analyzing events generated by the computer code FRITIOF based on the Lund Monte Carlo model for high-energy nucleus-nucleus interaction. The model assumes that, as two nucleons collide with each other particle production takes place through the creation of longitudinally excited strings between the constituents of the same nucleon that subsequently fragment, and new hadrons originate. The nucleus-nucleus collision is assumed to be a combination of multiple collisions between the nucleons belonging to one nucleus with those of the other. Large samples (7×10^4 for each interaction) of ^{16}O-emulsion and ^{32}S-emulsion events with minimum bias have been generated using the code, taking into account the proportional abundance of different target nuclei present in the emulsion material used in the experiment. ^{16}O-Ag/Br and ^{32}S-Ag/Br event samples having similar multiplicity distribution of shower particles as the corresponding experimental data set have been selected for analysis, though in each case the size of generated event samples was ten times as large as the experimental one.

A similar comparison of experimental results has also been made with event samples simulated by generating random numbers in place of phase space variable. The sample size is once again ten times the size of the experimental one, and the shower multiplicity distribution is the same as the experimental one. Independent emission of particles was assumed, as no correlation for particle production was input while generating the random numbers.

III. METHODOLOGY

The single-event factorial moment of order q is defined as

$$F_q^e = \frac{\frac{1}{M}\sum_{m=1}^{M} n_m(n_m-1)\cdots(n_m-q+1)}{\left(\frac{1}{M}\sum_{m=1}^{M} n_m\right)^q}, \tag{2}$$

where M is the pseudorapidity interval number and n_m is the number of particles falling within the mth interval in an event. By averaging F_q^e over the N number of events present in a particular sample one gets the so-called horizontally averaged scaled factorial moment

$$\langle F_q \rangle_H = \frac{1}{N}\sum_{e=1}^{N} F_q^e. \tag{3}$$

Whereas the horizontally averaged moment as defined here is sensitive to the shape of the single-particle density distribution and depends on the correlation between the cells, there exists another vertically averaged factorial moment [6], which is normalized locally and therefore carries information only about fluctuation within each cell.

The problem associated with the shape dependence of the single-particle density distribution can be taken care of either by introducing the Fialkowski correction factor [18] or by converting the phase space variable to a cumulative variable [19],

$$\chi(\eta) = = \int_{\eta_{\min}}^{\eta} \rho(\eta')d\eta' \Big/ \int_{\eta_{\min}}^{\eta_{\max}} \rho(\eta')d\eta', \tag{4}$$

such that irrespective of the basic phase space variable from which it is derived, the single-particle density distribution in terms of $\chi(\eta)$ is always uniform between 0 and 1. Such a uniformity of distribution is an implicit requirement of the

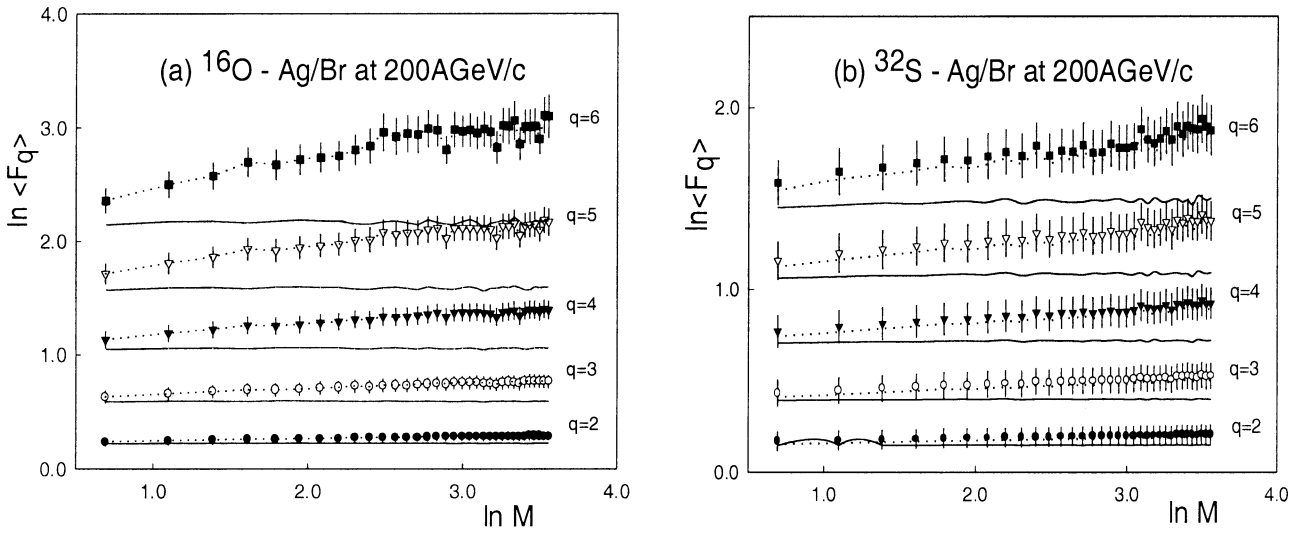

FIG. 1. Plot showing linear dependence of scaled factorial moments $\ln\langle F_q\rangle$ on $\ln M$ of order $q = 2$, 3, 4, 5, and 6 for (a) ^{16}O-Ag/Br interactions and (b) ^{32}S-Ag/Br interactions at 200 A GeV/c. Points with error bars are associated with the horizontally averaged scaled factorial moments, the dotted lines are for vertically averaged scaled factorial moments, and the solid lines represent horizontally averaged scaled factorial moments for generated data using the computer code FRITIOF.

power-law scaling behavior of the factorial moments,

$$\langle F_q\rangle_H \propto M^{\phi_q}, \tag{5}$$

where ϕ_q is called the intermittency index. Since F_q^e fluctuates to a large extent from event to event, a new normalized moment is introduced,

$$\Phi_q = F_q^e \big/ \langle F_q^e\rangle_H . \tag{6}$$

As $\langle F_q^e\rangle_H$ contains little statistical fluctuation one should therefore define the event-averaged pth-order moment of the normalized qth-order factorial moment as

$$C_{p,q} = \langle \Phi_q^p \rangle. \tag{7}$$

If one observes a generalized power-law dependence of $C_{p,q}$ on $g(M)$, a function of M, like

$$C_{p,q} \propto g(M)^{\Psi_q(p)}, \tag{8}$$

the phenomenon is referred to as erraticity of nonstatistical fluctuation, and $\Psi_q(p)$ is called the erraticity exponent. One can also define an entropy-like quantity,

$$\Sigma_q = \langle \Phi_q \ln \Phi_q \rangle. \tag{9}$$

The quantity Σ_q is related to the entropy index μ_q in the following way:

$$\Sigma_q \propto \mu_q \ln g(M), \tag{10}$$

provided $C_{p,q}$ exhibits a scaling behavior like Eq. (8). However, Σ_q does not really represent the entropy of the system defined in phase space, because it is defined over event space, which is not partitioned into smaller subintervals. We expect a linear dependence of Σ_q on Σ_2, with the slope for such a dependence being denoted by

$$\omega_q = \partial \Sigma_q / \partial \Sigma_2, \tag{11}$$

and it automatically follows that

$$\mu_q = \mu_2 \omega_q. \tag{12}$$

IV. DATA ANALYSIS AND RESULTS

Experimental results on intermittency analysis of shower track emissions in ^{16}O-Ag/Br and in ^{32}S-Ag/Br interactions are schematically presented in Figs. 1(a) and 1(b), respectively, with a plot of $\ln\langle F_q\rangle$ against $\ln M$ of order $q = 2$ to 6 in each case. In these diagrams the points represent horizontally averaged moments $\langle F_q\rangle_H$, the dotted lines are obtained by joining the points for vertically averaged moments $\langle F_q\rangle_V$, and the solid lines represent the FRITIOF prediction for $\langle F_q\rangle_H$. Because the factorial moments are computed for a uniformly distributed quantity like the cumulative variable $\chi(\eta)$, within statistical errors virtually no difference between the results obtained from two different averaging processes can be seen. Unlike in the experimental case, the FRITIOF values of factorial moments remain more or less uniform within statistical errors. When $\ln\langle F_q\rangle_H$ values are fitted against $\ln M$, reasonably good linear variation for each q value was obtained for both sets of experimental data. Thus a power-law scaling behavior as described in Eq. (5) is indeed obeyed by the experimentally obtained scaled factorial moments. The FRITIOF results exhibit only very little changes with changing M, and for random-number-generated events the $\ln\langle F_q\rangle_H$ values, which are not graphically plotted, actually showed a marginal decrease with increasing $\ln M$. The nature of linear dependences of $\ln\langle F_q\rangle_H$ on $\ln M$ is reflected in the values of intermittency indices ϕ_q listed in Table I, for both kinds of experimental data along with the respective FRITIOF and random-number predictions. From this table one can note that for ^{16}O-Ag/Br interactions ϕ_q values are consistently higher than the corresponding values for ^{32}S-Ag/Br interactions. This is consistent with the previous

TABLE I. Values of intermittency indices for ^{16}O-Ag/Br and ^{32}S-Ag/Br interactions at 200 A GeV/c.

Interaction	Data set	ϕ_2	ϕ_3	ϕ_4	ϕ_5	ϕ_6
^{16}O-Ag/Br	Experiment	0.018 ± 0.00058	0.048 ± 0.0016	0.091 ± 0.0036	0.15 ± 0.0073	0.24 ± 0.014
	FRITIOF	0.00039 ± 0.00026	0.0012 ± 0.00068	0.0029 ± 0.0013	0.0056 ± 0.0024	0.0078 ± 0.0042
	Random number	-0.005 ± 0.00037	-0.016 ± 0.0012	-0.032 ± 0.0024	-0.052 ± 0.0045	-0.076 ± 0.0079
^{32}S-Ag/Br	Experiment	0.013 ± 0.0003	0.032 ± 0.0008	0.056 ± 0.0018	0.082 ± 0.0035	0.112 ± 0.0056
	FRITIOF	0.00076 ± 0.00014	0.0023 ± 0.00040	0.0050 ± 0.00080	0.0093 ± 0.0014	0.015 ± 0.0022
	Random number	-0.0044 ± 0.00034	-0.014 ± 0.00095	-0.029 ± 0.0019	-0.05 ± 0.0034	-0.077 ± 0.0055

observations that, for a given order q, the more violent is the collision, the less is the value of intermittency index. At this point it is to be understood that the results of the one-dimensional intermittency analysis are included in the present investigation only for the sake of completeness, as one needs to evaluate the factorial moments first, before going into the erraticity analysis of data.

In Figs. 2(a) and 2(b) the frequency distributions of single-event factorial moments F_2^e in event space have been shown for $M = 5$ and 10, for both ^{16}O-Ag/Br and ^{32}S-Ag/Br interactions. The entire range of values of single-event factorial moments for a particular partition number M has been divided into a number of smaller groups, and the frequency distributions are obtained. Though the majority of the values of F_2^e are confined within a limited range, large values of F_2^e are also encountered in significant numbers in each case. It is these fluctuations in event space that can be quantified in terms of the erraticity moments and can be related to the chaotic behavior of multiparticle production dynamics.

In Figs. 3(a)–3(e) the eraticity moments $C_{p,q}$ are graphically plotted as a function of the partition number M for $q = 2$ to 6, and for $p = 0.5$, 0.9, 1.2, 1.4, and 1.6 for the experimental ^{16}O-Ag/Br interaction data. Corresponding FRITIOF predictions are shown in Figs. 3(f)–3(j). Similar schematic representations for ^{32}S-Ag/Br data are given in Figs. 4(a)–4(j). From these diagrams the following points may be noted. Because the relevant erraticity parameters can all be derived from the variation pattern of the erraticity moments in the neighborhood of $p = 1$, the analysis has been performed and the graphs are drawn only for that region. In general a nonlinear dependence of $\ln C_{p,q}(M)$ on $\ln M$ can be observed, a feature that is more prominent for moments with $p < 1$ than for moments with $p > 1$. For larger values of order of spatial fluctuation, that is, $q = 5$ or 6 and for $p > 1$, saturation effects in the values of $\ln C_{p,q}(M)$ can be seen in the higher M region for both experimental data sets. This feature can be attributed to a finite number of particles in an event, because with increasing M fewer events contribute to the moments of higher order. A few kinks can also be found in these plots, which are probably due to large event-to-event fluctuation in particle number in a particular bin. On average a heavy-ion event has larger shower multiplicity than a hadronic interaction at the same energy, and therefore in a heavy-ion event the bin-to-bin fluctuation of multiplicity is not as large as in a hadronic event. For each q, standard statistical errors due to event-to-event fluctuation of the scaled factorial moments associated with the data points are shown only for the highest and the lowest values of p. For the FRITIOF-generated events the pattern of variation of $\ln C_{p,q}(M)$ on $\ln M$ is more or less similar to that of the experiment, but the magnitudes of erraticity moments are always significantly less in both cases of generated events than in the experiment. In our work a generalized scaling form as given by Eq. (8) has been used. It was emphasized by Cao and Hwa [10] that a common function $g(M)$ may not always best represent the variation of $C_{p,q}(M)$ with M for all p and all q. Therefore, they suggested that a possible functional form for $g(M)$ can be $\ln g(M) = (\ln M)^b$, and $\ln C_{p,q}(q > 2)$ will automatically be linear against $\ln C_{2,2}$. The best linear dependence of $\ln C_{2,2}$ on $\ln g(M)$ can be obtained by adjusting the value of b. For ^{16}O-Ag/Br interactions this has been

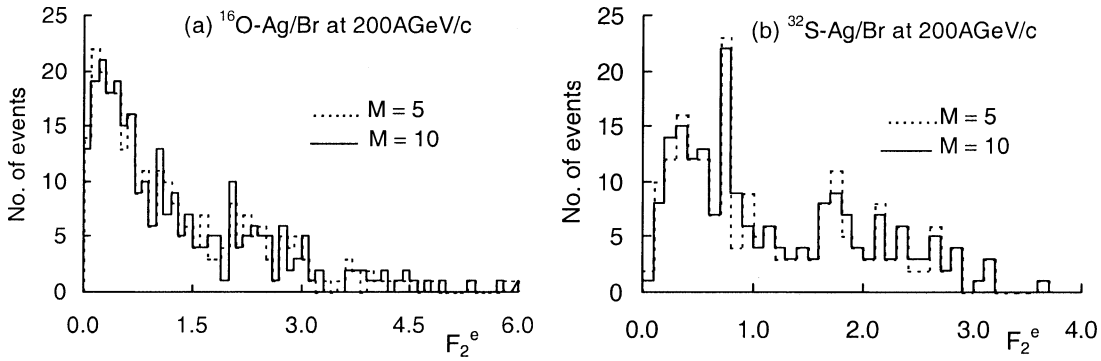

FIG. 2. Frequency distribution of single event factorial moments for different partition number M of order $q = 2$ for (a) ^{16}O-Ag/Br interactions and (b) for ^{32}S-Ag/Br interactions at 200 A GeV/c.

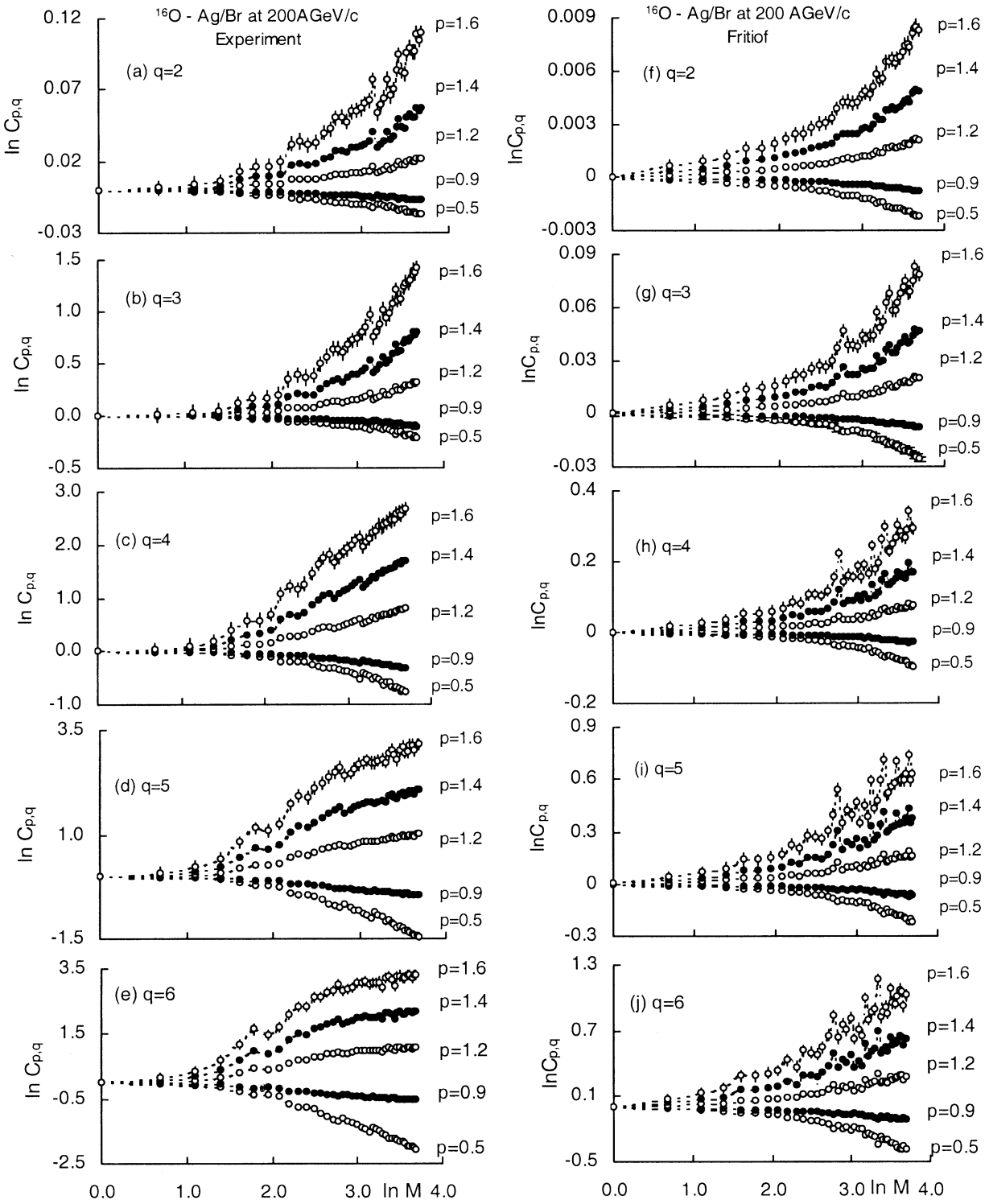

FIG. 3. Plot showing variation of $\ln C_{p,q}$ with $\ln M$ for $q = 2$ to 6, and for $p = 0.5$, 0.9, 1.2, 1.4, and 1.6, for both experimental and FRITIOF data sets for ^{16}O-Ag/Br interactions at 200 A GeV/c. Lines joining the points are drawn only to guide the eye.

achieved with $b = 3.225$ for the experiment, with $b = 3.04$ for the FRITIOF and $b = 4.02$ for the random-number-generated sample. Corresponding values for ^{32}S-Ag/Br interactions are, respectively, $b = 2.08$, 3.06, and 3.60.

In Figs. 5(a)–5(d) results of the best linear fit of $\ln C_{2,2}$ against $\ln g(M)$ for the experimental data sets, along with the corresponding FRITIOF predictions, are graphically plotted. From Eq. (8) one can readily see that in each case the slope of the linear variation of $\ln C_{2,2}$ on $\ln g(M)$ gives the value of the erraticity parameter $\psi_2(2)$. For ^{16}O-Ag/Br interactions, the values of $\psi_2(2)$ are listed in Table II for all three sets of data used in the present analysis. Corresponding

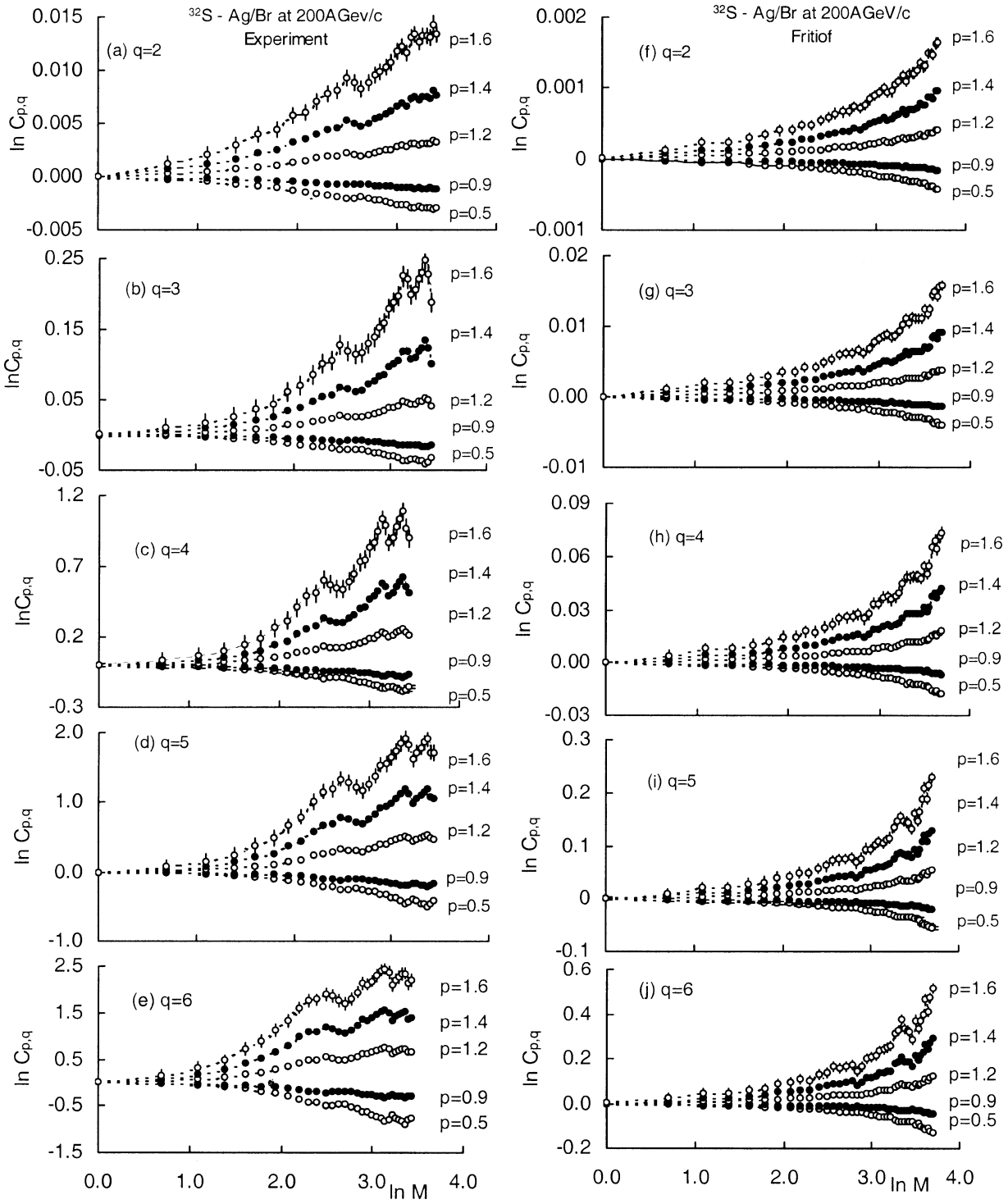

FIG. 4. Plot showing variation of $\ln C_{p,q}$ with $\ln M$ for $q = 2$ to 6, and for $p = 0.5$, 0.9, 1.2, 1.4, 1.6, for both experimental and FRITIOF data sets for ^{32}S-Ag/Br interactions at 200 A GeV/c. Lines joining the points are drawn only to guide the eye.

values for ^{32}S-Ag/Br interactions can be found in Table III.

As previously mentioned, instead of using $\ln M$ one can as well use $\ln C_{2,2}$ as the independent variable and hence obtain a linear dependence of $\ln C_{p,q}$ on $\ln C_{2,2}$. Such plots for both experimental data sets can be found in Figs. 6(a)–6(j) for $q = 2$ to 6, and for $p = 0.5$, 0.9, 1.2, 1.4, and 1.6. For the ^{16}O data, the linear dependence of $\ln C_{p,q}$ on $\ln C_{2,2}$ is good for $q = 2$ and 3, and for the ^{32}S data the goodness of linearity is acceptable until $q = 4$. Saturation effects are observed in the large $\ln C_{2,2}$ region for $q = 4$, 5, and 6, for ^{16}O; for ^{32}S-Ag/Br such effects are seen for $q = 5$ and 6.

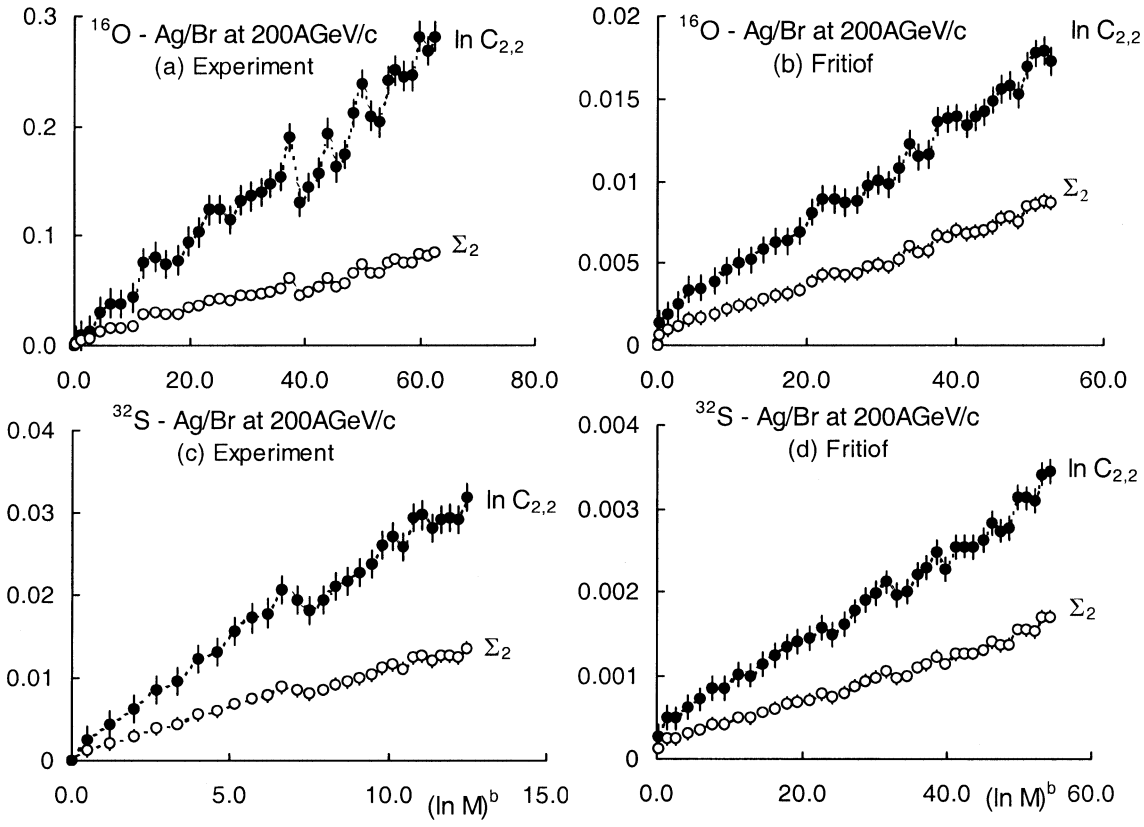

FIG. 5. Plot of $\ln C_{2,2}$ and Σ_2 against $(\ln M)^b$ for (a) ^{16}O-Ag/Br interactions at 200 A GeV/c, (b) FRITIOF results for ^{16}O-Ag/Br interactions, (c) ^{32}S-Ag/Br interactions at 200 A GeV/c, and (d) FRITIOF results for ^{32}S-Ag/Br interactions. Lines joining the points are drawn only to guide the eye.

In each case a linear dependence of $\ln C_{p,q}$ on $\ln C_{2,2}$ was obtained only within a limited region, for example, for ^{16}O data it was $0.09 < \ln C_{2,2} < 0.21$, and for ^{32}S data the range was $0.01 < \ln C_{2,2} < 0.02$. The corresponding range of phase space partition number in either case would be from $M = 10$ to 25. In all these cases the R^2 values obtained for the best linear regression between the independent and the dependent variables are close to 0.9 to ensure a reasonably good linear dependence between these variables. Therefore, one can conclude that a scaling behavior

TABLE II. Values of erraticity parameters for ^{16}O-Ag/Br imeractions at 200 A GeV/c.

Data set		χ'_q	ω_q	μ_q [Eq. (12)]	μ_q [Eq. (16)]
	$q=2$	0.34 ± 0.13	1.00 ± 0.00	$1.13 \times 10^{-3} \pm 3.48 \times 10^{-5}$	$1.3 \times 10^{-3} \pm 5.21 \times 10^{-4}$
	$q=3$	5.92 ± 0.24	16.22 ± 0.55	$1.84 \times 10^{-2} \pm 8.43 \times 10^{-4}$	$2.28 \times 10^{-2} \pm 1.38 \times 10^{-4}$
Experiment	$q=4$	18.87 ± 1.12	54.75 ± 1.853	$6.20 \times 10^{-2} \pm 2.84 \times 10^{-3}$	$7.26 \times 10^{-2} \pm 4.79 \times 10^{-3}$
	$q=5$	20.86 ± 0.06	72.74 ± 3.34	$8.24 \times 10^{-2} \pm 4.60 \times 10^{-3}$	$8.02 \times 10^{-2} \pm 2.34 \times 10^{-3}$
	$q=6$	18.51 ± 0.13	68.66 ± 4.26	$7.78 \times 10^{-2} \pm 5.38 \times 10^{-3}$	$7.12 \times 10^{-2} \pm 2.13 \times 10^{-3}$
	$q=2$	0.50 ± 0.01	1.00 ± 0.00	$1.50 \times 10^{-4} \pm 2.43 \times 10^{-6}$	$1.50 \times 10^{-4} \pm 3.86 \times 10^{-6}$
	$q=3$	4.88 ± 0.06	9.82 ± 0.12	$1.48 \times 10^{-3} \pm 3.00 \times 10^{-5}$	$1.47 \times 10^{-3} \pm 2.95 \times 10^{-5}$
FRITIOF	$q=4$	18.41 ± 0.05	37.02 ± 0.49	$5.57 \times 10^{-3} \pm 1.16 \times 10^{-4}$	$5.53 \times 10^{-3} \pm 9.24 \times 10^{-5}$
	$q=5$	41.44 ± 0.06	84.47 ± 1.40	$1.27 \times 10^{-2} \pm 2.93 \times 10^{-4}$	$1.25 \times 10^{-2} \pm 2.05 \times 10^{-4}$
	$q=6$	67.32 ± 0.53	148.40 ± 3.34	$2.23 \times 10^{-2} \pm 6.18 \times 10^{-4}$	$2.02 \times 10^{-2} \pm 3.71 \times 10^{-4}$
	$q=2$	0.53 ± 0.073	1.00 ± 0.00	$4.86 \times 10^{-5} \pm 1.15 \times 10^{-7}$	$4.90 \times 10^{-5} \pm 6.81 \times 10^{-6}$
Random	$q=3$	4.91 ± 0.76	8.93 ± 0.19	$4.34 \times 10^{-4} \pm 1.38 \times 10^{-5}$	$4.43 \times 10^{-4} \pm 6.91 \times 10^{-5}$
number	$q=4$	17.53 ± 0.08	33.77 ± 0.81	$1.64 \times 10^{-3} \pm 5.60 \times 10^{-5}$	$1.58 \times 10^{-3} \pm 3.92 \times 10^{-5}$
	$q=5$	36.84 ± 0.03	73.73 ± 2.70	$3.58 \times 10^{-3} \pm 1.58 \times 10^{-4}$	$3.32 \times 10^{-3} \pm 8.08 \times 10^{-5}$
	$q=6$	77.38 ± 0.11	133.00 ± 2.28	$6.46 \times 10^{-3} \pm 1.92 \times 10^{-4}$	$6.99 \times 10^{-3} \pm 1.70 \times 10^{-4}$

TABLE III. Values of erraticity parameters for ^{32}S-Ag/Br interactions at 200 *A* GeV/*c*.

Data set		χ'_q	ω_q	μ_q [Eq. (12)]	μ_q [Eq. (16)]
Experiment	$q=2$	0.44 ± 0.05	1.00 ± 0.00	$1.26 \times 10^{-3} \pm 2.90 \times 10^{-5}$	$1.27 \times 10^{-3} \pm 1.60 \times 10^{-4}$
	$q=3$	7.06 ± 1.74	15.55 ± 0.538	$1.95 \times 10^{-2} \pm 8.00 \times 10^{-4}$	$2.05 \times 10^{-2} \pm 5.10 \times 10^{-3}$
	$q=4$	33.98 ± 3.17	79.63 ± 3.33	0.10 ± 0.0048	0.099 ± 0.0095
	$q=5$	72.26 ± 17.37	191.20 ± 4.998	0.24 ± 0.0084	0.21 ± 0.051
	$q=6$	101.07 ± 25.68	282.7 ± 7.529	0.36 ± 0.0125	0.293 ± 0.075
FRITIOF	$q=2$	0.497 ± 0.003	1.00 ± 0.00	$2.63 \times 10^{-5} \pm 4.89 \times 10^{-7}$	$2.63 \times 10^{-5} \pm 5.01 \times 10^{-7}$
	$q=3$	4.76 ± 0.11	9.48 ± 0.086	$2.49 \times 10^{-4} \pm 5.16 \times 10^{-6}$	$2.52 \times 10^{-4} \pm 5.57 \times 10^{-6}$
	$q=4$	21.61 ± 1.375	42.42 ± 0.7655	$1.12 \times 10^{-3} \pm 2.89 \times 10^{-5}$	$1.15 \times 10^{-3} \pm 4.22 \times 10^{-5}$
	$q=5$	65.47 ± 4.953	127.7 ± 2.998	$3.36 \times 10^{-3} \pm 1.00 \times 10^{-4}$	$3.47 \times 10^{-3} \pm 1.60 \times 10^{-4}$
	$q=6$	149.5 ± 3.893	292.4 ± 7.604	$7.69 \times 10^{-3} \pm 2.50 \times 10^{-4}$	$7.93 \times 10^{-3} \pm 1.80 \times 10^{-4}$
Random number	$q=2$	0.492 ± 0.006	1.00 ± 0.00	$1.43 \times 10^{-5} \pm 5.56 \times 10^{-7}$	$1.43 \times 10^{-5} \pm 6.10 \times 10^{-7}$
	$q=3$	4.66 ± 0.171	9.373 ± 0.113	$1.34 \times 10^{-4} \pm 5.40 \times 10^{-6}$	$1.36 \times 10^{-4} \pm 7.40 \times 10^{-6}$
	$q=4$	21.64 ± 2.096	43.08 ± 0.7322	$6.17 \times 10^{-4} \pm 2.60 \times 10^{-5}$	$6.31 \times 10^{-4} \pm 6.60 \times 10^{-5}$
	$q=5$	67.74 ± 7.125	134.90 ± 2.905	$1.93 \times 10^{-3} \pm 8.60 \times 10^{-5}$	$1.97 \times 10^{-3} \pm 2.20 \times 10^{-4}$
	$q=6$	154.00 ± 7.81	305.0 ± 7.24	$4.37 \times 10^{-3} \pm 1.99 \times 10^{-4}$	$4.49 \times 10^{-3} \pm 2.90 \times 10^{-4}$

such as

$$C_{p,q} \propto (C_{2,2})^{\chi(p,q)} \tag{13}$$

is obeyed by the erraticity moments. For each q and for different p values, the exponents $\chi(p,q)$ are obtained from the best linear dependence of $\ln C_{p,q}$ against $\ln C_{2,2}$, and thereafter these values are fitted with a quadratic function of p such as

$$\chi(p,q) = \alpha_q p^2 + \beta_q p + \gamma_q. \tag{14}$$

The derivatives of such quadratic functions at $p=1$,

$$\chi'_q = \frac{d}{dp}\chi(p,q)|_{p=1}, \tag{15}$$

will give us another erraticity parameter, values of which are listed in Tables II and III, respectively, for ^{16}O-Ag/Br and ^{32}S-Ag/Br interactions.

We are now in a position to derive the entropy index μ_q from the following relation:

$$\mu_q = \psi_2(2)\chi'_q. \tag{16}$$

The values of μ_q are also given in Tables II and III. As has been pointed out in Sec. III, one can derive the μ_q values in a different way by making use of Eq. (12). Keeping in mind that $\ln g(M) = (\ln M)^b$ and setting the values of b as obtained before, one can obtain a linear dependence of Σ_2 against $\ln g(M)$. Along with $\ln C_{2,2}$, the variation of Σ_2 against $\ln g(M)$ has been included in Figs. 5(a)–5(d) for both ^{16}O-Ag/Br and ^{32}S-Ag/Br experimental data sets, as well as for the corresponding FRITIOF data sets. The slopes of these straight lines directly provide us with the values of μ_2. As expected, Σ_q should linearly rise with Σ_2 . Graphical plots showing variation of Σ_q on Σ_2 is presented in Figs. 7(a)–7(d). For $q=5$ and 6, saturation effects are observed for the ^{16}O-Ag/Br experimental data, which is absent for the ^{32}S-Ag/Br interactions. Slopes of the best-fitted straight lines (ω_q) obtained from these graphs were used to derive μ_q from Eq. (12). The values of ω_q and μ_q are also given in Tables II and III.

In Figs. 8(a)–8(h) the values of all erraticity parameters—χ'_q, ω_q, and μ_q—have been graphically plotted against order number q for both types of interactions and for all three data sets, that is, experimental, FRITIOF, and random number. For the FRITIOF and random-number-generated events, the variation patterns of all erraticity parameters are more or less similar. As expected the experimental results show different trends. A closer look at these graphs shows that the χ'_q and ω_q values for both kinds of generated data and both types of interaction increase systematically with q, whereas the corresponding experimental values, after showing a similar initial trend, differ significantly from the generated results in the higher q region, that is, for $q=5$ and 6 for ^{16}O and for $q=6$ for ^{32}S events. For ^{16}O the experimental values of χ'_q saturate at a higher q region, which is not the case for ^{32}S. The other parameter, ω_q, again shows significant difference between generated and experimental results only at $q=6$ for the ^{16}O data, whereas for ^{32}S small differences exist at $q=4$ and 5. This parameter saturates at higher q only for the experimental data of the ^{16}O interaction, and in all other cases it systematically increases with q. For both types of interactions large differences can be observed in the variation of the entropy index μ_q with q between the generated data and the experimental data.

Values of entropy indices obtained from the FRITIOF and random-number-generated samples in either of the interactions change similarly, showing a marginal increase with increasing q, as can be seen from Figs. 4(c), 4(d), 4(g), and 4(h). The experimentally obtained values μ_q for the ^{32}S event sample are consistently higher than the corresponding values of the ^{16}O event sample. Besides an initial

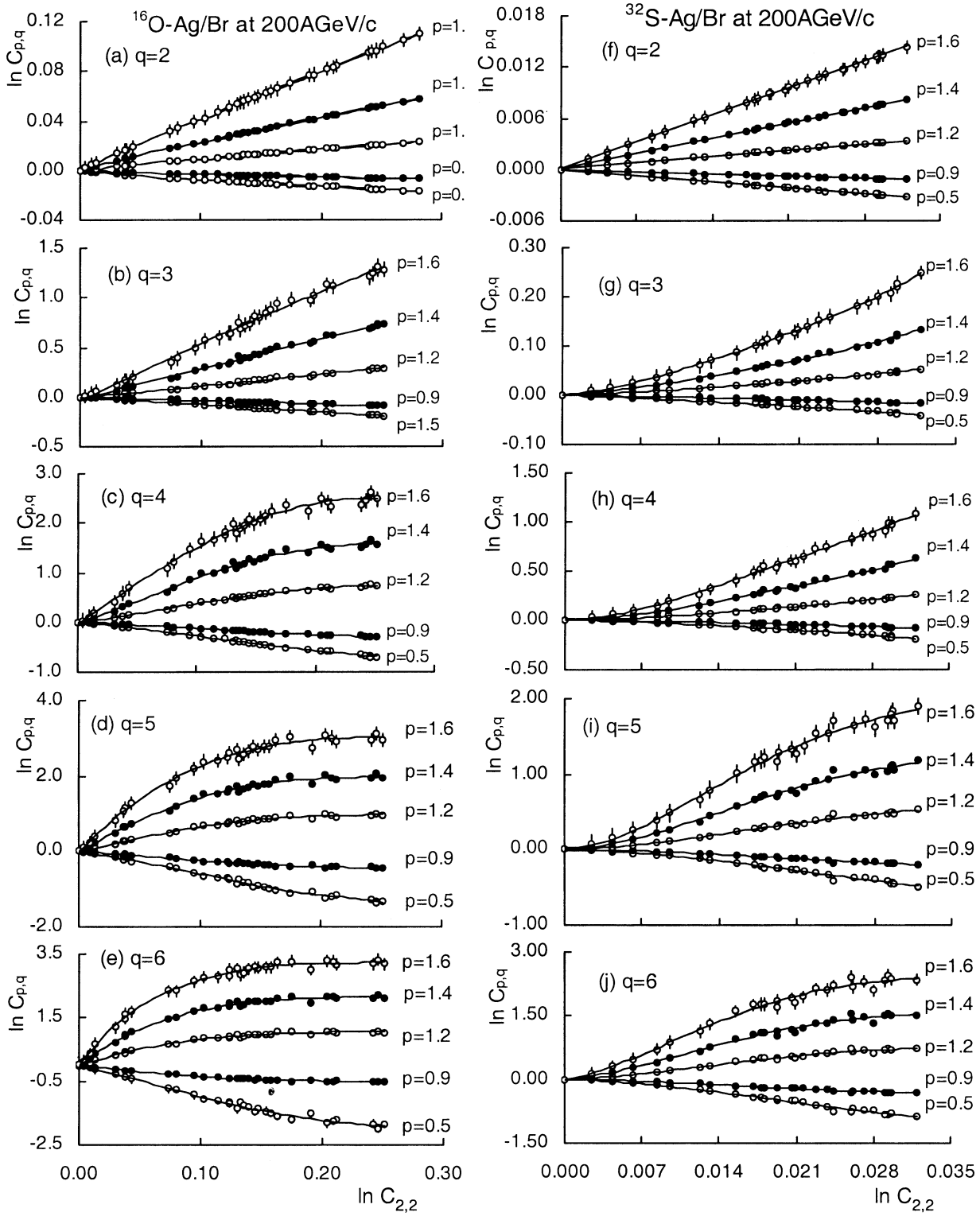

FIG. 6. Plot showing dependence of $\ln C_{p,q}$ on $\ln C_{2,2}$ for $q = 2$ to 6, and for $p = 0.5, 0.9, 1.2, 1.4$, and 1.6, for (a)–(e) ^{16}O-Ag/Br interactions at 200 A GeV/c, and (f)–(j) ^{32}S-Ag/Br interactions at 200 A GeV/c. Curves are drawn to guide the eye.

increasing trend, saturation effects can be observed in the experimental data on ^{16}O induced interactions around $q = 5$ and 6, which are absent for the corresponding ^{32}S data, possibly owing to a lesser average shower multiplicity in the former case. Within statistical uncertainties, values of μ_q calculated in two quite different ways [i.e., either using Eq. (12) or Eq. (16)] reasonably agree with each other.

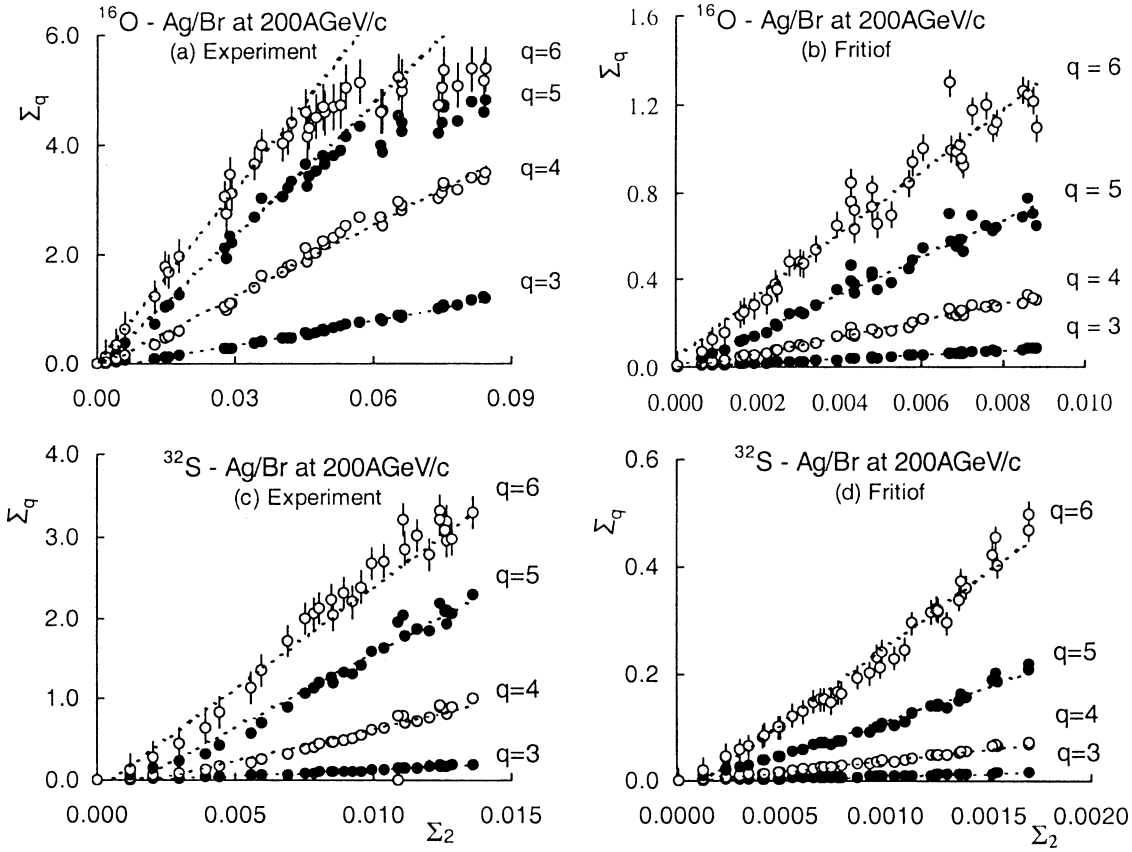

FIG. 7. Plot of Σ_q against Σ_2 for $q = 3$ to 6 for (a) ^{16}O-Ag/Br interactions at 200 A GeV/c, (b) FRITIOF results for ^{16}O-Ag/Br interactions, (c) ^{32}S-Ag/Br interactions at 200 A GeV/c, and (d) FRITIOF results for ^{32}S-Ag/Br interactions. In each case, the dashed lines represent the best straight-line fit only for the linear portion of the graph.

V. DISCUSSION

From the preceding analysis on intermittency it can now be concluded that spatial fluctuations of dynamical origin are present in the phase space distribution of charged particles produced in ^{16}O-Ag/Br and ^{32}S-Ag/Br interactions at 200 A GeV/c. Fluctuations in the density distribution of like-sign charged particles in small intervals of phase space can be explained in terms of Bose-Einstein (BE) correlation (i.e., interference among identical particles emitted by an extended coherent source). For shower tracks, which are created by both positive and negative charges (mostly pions), the increase of scaled factorial moments with decreasing interval size shows a small but significant effect beyond the BE correlation effect. Such intermittency effects are not observed in the event samples generated either by the Lund Monte Carlo code FRITIOF or by random numbers. The lower values of intermittency indices in experiments involving higher mass number or energy of the incident nucleus have been explained in terms of intermixing of more sources of particle production within the collision region [6,7]. We would like to point out that more rigorous analysis of intermittency in a higher dimension of phase space should be performed to draw any stronger conclusion.

The erraticity analysis shows the signature of chaotic behavior of spatial fluctuation in multiparticle production in both ^{16}O-Ag/Br and ^{32}S-Ag/Br interactions. A substantial amount of event-to-event fluctuations of factorial moments are observed in the experiments. The fluctuations resulted in a power-law scaling variation of the erraticity moments $C_{p,q}$ and Σ_q. The results of each generated data set significantly differ from the corresponding experimental one, and we conclude that the entropy index μ_q is the most suitable parameter to compare experimental results with model predictions, as it amply reflects the inadequacy of model predictions in our case. Neither an independent emission model nor a string fragmentation mechanism of particle production can account for the variation of μ_q for the present set of data. Although the effects of two-particle correlation have been taken into consideration in FRITIOF, such effects cannot completely account for the outcome of heavy-ion interactions, as can be seen from the similar intermittency results in FRITIOF and random number event samples. Therefore it is not surprising that FRITIOF also fails to predict the observed event-to-event fluctuation of scaled factorial moments, as in this regard no dynamical input has been introduced into the code. Consequently, the FRITIOF predictions are similar to those obtained from random numbers. This suggests that the

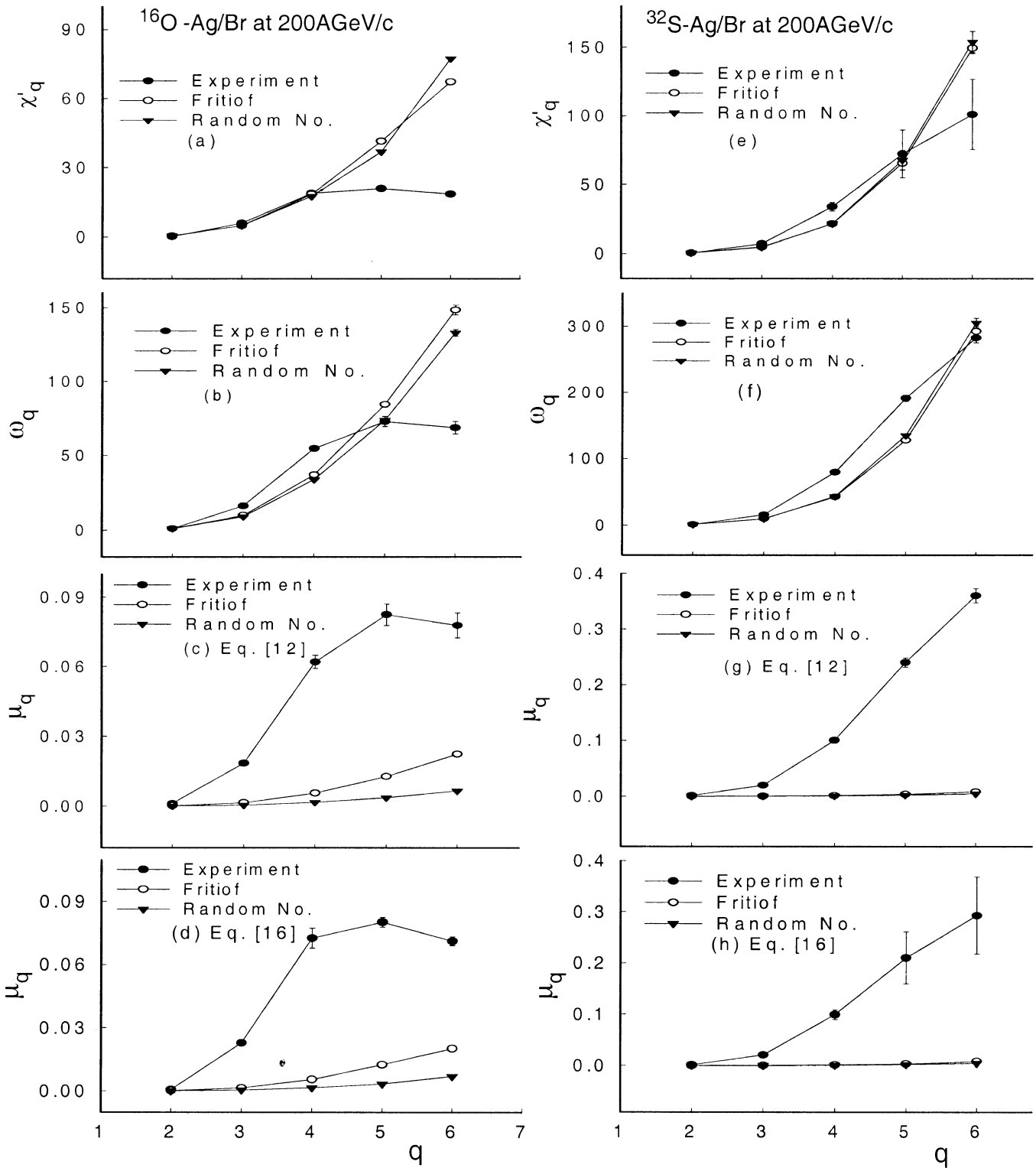

FIG. 8. Plot of erraticity parameters against order number q. Two different plots for the entropy index (μ_q) are shown for two equations used to derive its value.

QCD branching processes associated with particle production are more chaotic for each experiment than for both of the corresponding generated data sets. The observed fluctuations of scaled factorial moments need to be addressed with new physics as input. The experimental values of the erraticity parameters given in Tables II and III may be used for this purpose. However, in the present case experimental values of μ_q are significantly smaller than those involving hadrons and

nucleons [10–14]. This indicates that there is more fluctuation of F_q^e in event space for the present set of experimental data than in any other hadronic or nuclear collision. Since the emulsion data do not allow us to make a transverse momentum cut in the pseudorapidity distribution of produced particles, it is not possible at this stage to decide whether or not some kind of phase transition is responsible for such fluctuations.

ACKNOWLEDGMENTS

The authors express their gratefulness to Prof. P. L. Jain of SUNY at Buffalo, USA, and to Prof. D. Ghosh of Jadavpur University, Kolkata, India, respectively, for providing the nuclear emulsion plates and allowing use of the laboratory infrastructure. The authors are also thankful to the IUCAA Reference Centre of the University of North Bengal for making its Internet facilities available.

[1] JACEE Collaboration, T. H. Burnet *et al*., Phys. Rev. Lett. **50**, 2062 (1983).
[2] A. Bialas and R. Peschanski, Nucl. Phys. **B273**, 703 (1986); **B308**, 857 (1988).
[3] B. Buschbech, R. Lipa, and R. Peschanski, Phys. Lett. **B215**, 788 (1988); W. Braunscheweig *et al*., *ibid.* **B231**, 548 (1989).
[4] EM Collaboration, I. Derado, G. Jansco, N. Schmitz, and P. Stopa, Z. Phys. C **47**, 23 (1990).
[5] NA22 Collaboration, I. V. Ajinenko *et al*., Phys. Lett, **B222**, 306 (1989).
[6] KLM Collaboration, R. Holynski *et al*., Phys. Rev. Lett. **62**, 733 (1989); EMU-01 Collaboration, M. I. Adamovich *et al*., Phys. Lett. **B263**, 539 (1991); Nucl. Phys. **B388**, 3 (1992).
[7] E. A. De Wolf, I. M. Dremin, and W. Kittel, Phys. Rep. **270**, 1 (1996).
[8] R. C. Hwa, Phys. Lett. **B201**, 165 (1988); I. M. Dremin, JETP Lett. **30**, 152 (1980); Sov. J. Nucl. Phys. **33**, 726 (1981); W. Ochs and J. Wosiek, Phys. Lett. **B214**, 617 (1988); B. Andersson, P. Dahlquist, and G. Gustarson, *ibid.* **B214**, 604 (1988); B. C. Chiu and R. C. Hwa, *ibid.* **B236**, 466 (1990).
[9] Z. Cao and R. C. Hwa, Phys. Rev. Lett. **75**, 1268 (1995); Phys. Rev. D **53**, 6608 (1996); Phys. Rev. E **56**, 326 (1997).
[10] Z. Cao and R. C. Hwa, Phys. Rev. D **61**, 074011 (2000).
[11] EHS/NA22 Collaboration, M. R. Atayan *et al*., University of Nijmegen internal publications, HEN 449 (2003).
[12] W. Shaoshun and W. Zhaomin, Phys. Rev. D **57**, 5 (1998).
[13] F. Jinghua, W. Yuanfang, and L. Lianshou, HZPP-9903 (1999); F. Jinghua, L. Lianshou, and W. Yuanfang, HZPP-9901 (1999).
[14] D. Ghosh *et al*., Phys. Lett. **B540**, 52 (2002).
[15] M. K. Ghosh and A. Mukhopadhyay, Phys. Rev. C **68**, 034907 (2003).
[16] B. Anderson, G. Gustavson, and B. Nilsson-Almqvist, Nucl. Phys. **B281**, 289 (1987); B. Nilsson-Almqvist and E. Stenlund, Comput. Phys. Commun. **43**, 387 (1987).
[17] C. F. Powell, P. H. Fowler, and D. H. Perkins, *The Study of Elementary Particles by Photographic Method* (Pergamon, Oxford, 1959).
[18] K. Fialkowski *et al*., Acta Phys. Pol. B **20**, 639 (1989).
[19] A. Bialas and M. Gradzicki, Phys. Lett. **B252**, 483 (1990).